Nanoscale Res Lett (2009) 4:655–664
DOI 10.1007/s11671-009-9296-8

NANO EXPRESS

Influence of Matrix Polarity on the Properties of Ethylene Vinyl Acetate–Carbon Nanofiller Nanocomposites

Jinu Jacob George · Anil K. Bhowmick

Received: 8 December 2008 / Accepted: 5 March 2009 / Published online: 21 March 2009

Abstract A series of ethylene vinyl acetate (EVA) nanocomposites using four kinds of EVA with 40, 50, 60, and 70 wt% vinyl acetate (VA) contents and three different carbon-based nanofillers—expanded graphite (EG), multi-walled carbon nanotube (MWCNT), and carbon nanofiber (CNF) have been prepared via solution blending. The influence of the matrix polarity and the nature of nanofillers on the morphology and properties of EVA nanocomposites have been investigated. It is observed that the sample with lowest vinyl acetate content exhibits highest mechanical properties. However, the enhancement in mechanical properties with the incorporation of various nanofillers is the highest for EVA with high VA content. This trend has been followed in both dynamic mechanical properties and thermal conductivity of the nanocomposites. EVA copolymer undergoes a transition from partial to complete amorphousness between 40 and 50 wt% VA content, and this changes the dispersion of the nanofillers. The high VA-containing polymers show more affinity toward fillers due to the large free volume available and allow easy dispersion of nanofillers in the amorphous rubbery phase, as confirmed from the morphological studies. The thermal stability of the nanocomposites is also influenced by the type of nanofiller.

Keywords Nanocomposites · Carbon fillers · Ethylene vinyl acetate · Elastomers · Mechanical properties

J. J. George · A. K. Bhowmick (✉)
Rubber Technology Centre, Indian Institute of Technology, Kharagpur 721302, India
e-mail: anilkb@rtc.iitkgp.ernet.in

Introduction

Ethylene vinyl acetate (EVA) is one of the important organic polymers, extensively used for electrical insulation, cable jacketing and repair, component encapsulation and water proofing, corrosion protection, and packaging of components. However, bulk EVA does not often fulfill the requirements in terms of its thermal stability and mechanical properties in some specific areas. Studies have been reported on the effect of electron beam irradiation on the mechanical properties and thermal stability of the EVA elastomer [1, 2]. Also, in order to improve various properties, nanoparticles are added as fillers. Various research investigations have been reported on the properties of nanoclay-filled EVA nanocomposites [3–5]. Costache et al. [6] have worked on the thermal degradation behavior of EVA–clay nanocomposites. Studies have been reported on the linear viscoelastic behavior of EVA-layered silicate nanocomposites [7, 8]. Effect of vinyl acetate (VA) content on the mechanical and thermal properties of EVA/MgAl-layered double hydroxide nanocomposites has been studied by various groups [9, 10]. Several studies have focussed on the influence of VA content on the dispersion of clay platelets, addition of external compatibilizers [11, 12], or the nature of the clay organo-modifier [9]. Preparation and characterization of natural rubber (NR)/EVA blend–clay nanocomposites have also been reported in the literature [13]. Silica nanoparticles prepared through the sol–gel mechanism by hydrolysis of tetraethoxysilane (TEOS) are found to improve the gas barrier properties of EVA–silica nanocomposites membranes [14].

EVA is a random copolymer consisting of ethylene and vinyl acetate as repeating units. VA content has two fundamental effects that influence the properties of EVA copolymers. The first effect is to disrupt the crystalline

regions formed by the polyethylene segments of the copolymer. The second overriding effect of VA content results from the polar nature of the acetoxy side chain. The EVA shows various properties by varying the VA content. The properties of EVA depend on the crystallinity of the EVA [15–18], which can be controlled by the VA content.

Elastomers are proved to be very compatible matrices for carbon-based fillers. Several applications of rubbers might benefit from the incorporation of carbon nanofillers to form rubber-based nanocomposites. Studies have been carried out on the effect of carbon-based nanofillers on various properties of EVA thermoplastic elastomers having low VA content (25–32%), by melt mixing techniques [19–22]. From our laboratory, we have reported preliminary studies on the effect of various carbon-based nanofillers on the properties of elastomeric grade EVA [23–25]. However, there is no study carried out so far on the effect of VA content on the properties of these nanocomposites. Lee and Kim [21] describe the process of manufacturing nanocomposite material, which involves adding CNTs to improve EVA's physical characteristics such as radiation resistance and thermal properties. Effect of MWCNT on the fire retardant and electromagnetic interference shielding properties of EVA has been investigated by various groups [22, 26]. Effect of VA content on the properties of MWCNT-filled thermoplastic elastomeric EVA nanocomposites has also been reported in the literature [27].

This study aims at evaluating the effect of the VA content in elastomeric grade EVA copolymers, on the dispersion states of three different carbon nanofillers: expanded graphite (EG), multiwalled carbon nanotubes (MWCNTs), and carbon nanofibers (CNFs) and also on the morphological, mechanical, dynamic mechanical, and thermal properties of the resulting nanocomposites. The effect of polarity of the EVA matrix on the extent of dispersion and distribution of the carbon-based nanofillers has been investigated by solution blending of 4 wt% of these three fillers with four EVA matrices containing 40, 50, 60, and 70% VA units. These studies have not been reported in the literature.

Experimental

Materials

Four commercial ethylene vinyl acetate copolymer grades were supplied by Bayer (now Lanxess), Germany. The expanded graphite was procured from Asbury Graphite Mills Inc, NJ, USA. MWCNT was provided by Helix Material Solutions, TX, USA. CNF (as grown grade PR-24 AG, Pyrograf-III^{TM}) was obtained from Applied Sciences Inc., OH, USA. The dicumyl peroxide (DCP, 99% pure), cross-linker for the rubber, was obtained from Hercules India. Triallyl cyanurate (TAC), the co-crosslinker was procured from Fluka A G, Germany. Tetrahydrofuran (THF) of LR grade, used as the solvent for EVA was obtained from MERCK (India) Ltd., Mumbai, India.

Preparation of Nanocomposites

The nanocomposites were synthesized by using a solution-mixing technique. EVA (5 g per batch) was dissolved in 50 mL of THF to make 10% solution of the rubber using a mechanical stirrer. DCP (0.05 g) as the curing agent and 0.05 g of TAC as the co-agent were added to the rubber solution. The solution was thoroughly stirred using a mechanical stirrer. The nanofiller dispersed in THF was first sonicated for 15 min and subsequently added to the rubber solution while stirring at room temperature (27 °C). The final solution was cast over teflon trays and kept for air drying followed by vacuum drying at 50 °C, till there was practically no weight variation. The dried films were molded in a hot press at a pressure of 5 MPa at 150 °C for an optimum cure time of 25 min, determined from a Monsanto oscillating disc rheometer (ODR, 100S).

The various sample designations are given in Table 1.

Morphological Study

The microscopy was performed using a JEOL JEM-2010 (Japan), Transmission Electron Microscope (TEM) operating at an accelerating voltage of 200 kV. The composite samples were cut by ultra-cryomicrotomy using a Leica Ultracut UCT. Freshly sharpened glass knives with cutting edge of 45° were used to get the cryosections of 50–70 nm thickness. Since these samples were elastomeric in nature, the temperature during ultra-cryomicrotomy was kept at −50 °C (which was well below the glass transition temperature of EVA). The cryosections were collected individually on sucrose solution and directly supported on a copper grid of 300-mesh size.

Table 1 Sample designations for various nanocomposites

Sample designation	Description
EVA_{40}	Virgin EVA elastomer with 40% VA content
EVA_{50}	Virgin EVA elastomer with 50% VA content
EVA_{60}	Virgin EVA elastomer with 60% VA content
EVA_{70}	Virgin EVA elastomer with 70% VA content
EVA-4EG	EVA filled with 4 wt% of EG
EVA-4T	EVA filled with 4 wt% of MWCNT
EVA-4F	EVA filled with 4 wt% of CNF

Mechanical Property Analysis

The mechanical properties of the nanocomposites were evaluated by a universal testing machine (UTM, Zwick 1445) on dumbbell specimens, punched out from the cast films using an ASTM Die C. All the tests were carried out as per ASTM D 412-99 method at 25 ± 2 °C at a cross-head speed of 500 mm/min. The average values of three tests for tensile strength, tensile modulus, and elongation at break are reported for each sample.

Swelling Study

The swelling studies of the rubber specimens were carried out in toluene at ambient conditions (25 ± 2 °C) for 72 h. Volume fraction of rubber, V_r was calculated using the following equation [28]

$$V_r = \frac{(D - FT)\rho_r^{-1}}{(D - FT)\rho_r^{-1} + A_0\rho_s^{-1}} \quad (1)$$

where, V_r is volume fraction of rubber in the swollen gel, D the de-swollen weight of the composites, F the fraction insoluble, T the initial weight of the sample, and A_0 the amount of solvent imbibed. ρ_r is the density of the rubber, while ρ_s is density of the swelling solvent.

Differential Scanning Calorimetry (DSC)

DSC of various samples was carried out by using a Q-100 DSC, of TA instruments, USA. The test was carried out in the temperature range −100 to +100 °C, with samples of 5 mg weight and the rate of heating/cooling was fixed at 10 °C/min in nitrogen.

Dynamic Mechanical Thermal Analysis (DMTA)

Dynamic mechanical thermal characteristics of the composite films (0.4–0.6 mm thick) were evaluated by using a DMTA IV (Rheometric Scientific) under tension mode. All the data were analyzed using RSI Orchestrator application software on an ACER computer attached to the machine. The temperature sweep measurements were made from −35 to 20 °C. The experiments were carried out at a frequency of 1 Hz at a heating rate of 2 °C/min. The storage modulus (E') and the loss tangent (tan δ) data were recorded for all the samples under identical conditions.

Thermal Conductivity

The thermal conductivity of the various nanocomposites was measured as per ASTM C177-97. The thermal conductivity was calculated using the equation

$$K = \frac{Wt}{A\mathrm{d}T} \quad (2)$$

where W is the power in watts (here 4 W), K is the thermal conductivity, t the thickness of sample, A the area of the sample, and dT the temperature difference between the two plates.

Thermal Degradation Studies

Thermal stability of the composites was investigated by thermogravimetric analysis (TGA) by using a Perkin Elmer TGA instrument [Model: Pyris Diamond TG/DTA] from ambient to 800 °C at a programed heating rate of 20 °C/min in nitrogen. A sample weight of approximately 10 mg was taken for all the measurements. The weight loss against temperature was recorded. Differential thermogravimetric analysis (DTG) of the composites was represented in terms of the first derivative plots of the TGA curves. The data points denote the weight loss/time against temperature at the specified heating rate.

Results and Discussion

Morphological Analysis

Figure 1a–d displays the TEM images of the nanocomposites which show the distribution of EG in all the four EVA grades. The graphite flakes are distributed well in the elastomeric EVA matrices, with the presence of few filler aggregations in all the samples.

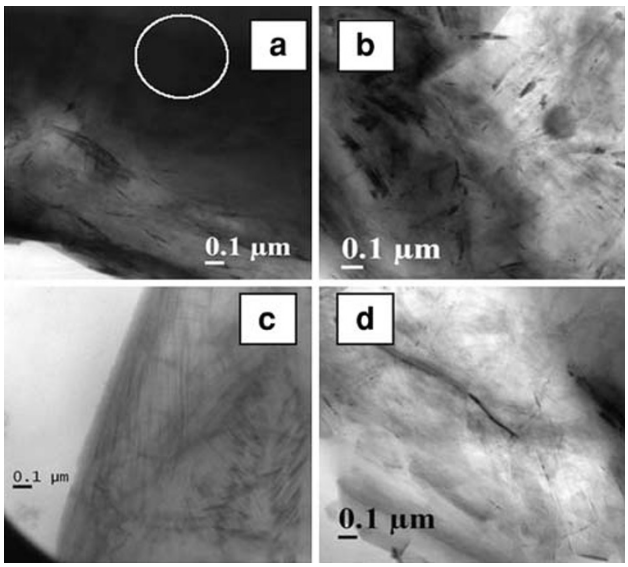

Fig. 1 TEM photographs of **a** EVA_{40}-4EG, **b** EVA_{50}-4EG, **c** EVA_{60}-4EG, and **d** EVA_{70}-4EG

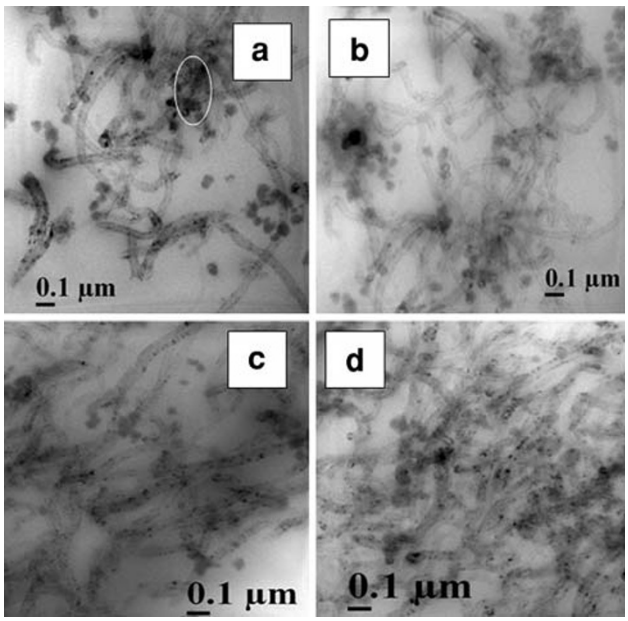

Fig. 2 TEM photographs of **a** EVA_{40}-4T, **b** EVA_{50}-4T, **c** EVA_{60}-4T, and **d** EVA_{70}-4T

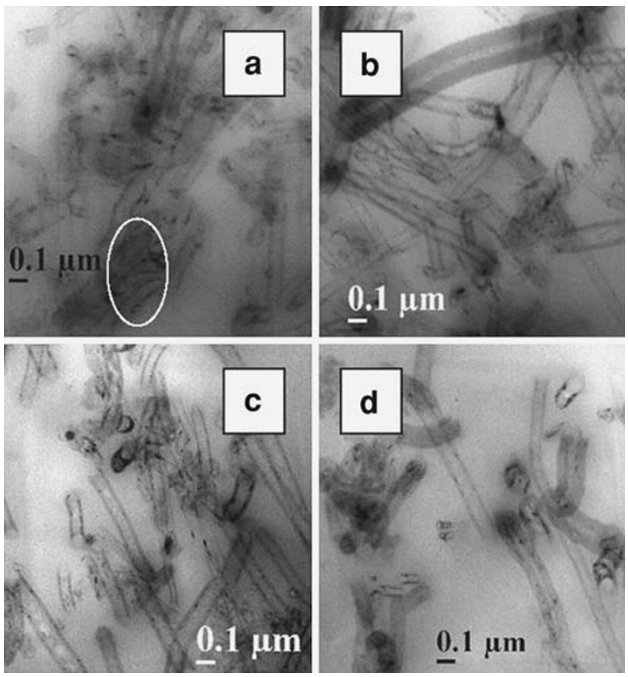

Fig. 3 TEM photographs of **a** EVA_{40}-4F, **b** EVA_{50}-4F, **c** EVA_{60}-4F, and **d** EVA_{70}-4F

A similar trend is observed in the case of EVA grades reinforced with MWCNT (Fig. 2a–d) and CNF as well (Fig. 3a–d). MWCNT is distributed relatively well in all the four matrices with the presence of small agglomerations. The CNFs are well dispersed in EVA and have an average diameter of 120 nm. The nanofillers show more affinity toward the rubber phase and are better dispersed there due to the large free volume available in the amorphous rubber phase. Hence, the high VA-containing grades show more uniform morphology. In EVA_{40}, all the nanofillers tend to form agglomerations (shown by circles in the figures).

Mechanical Properties

The tensile properties of various EVA samples and their 4 wt% filler loaded nanocomposites are plotted against the VA content. These are displayed in Fig. 4a–c. The presence of the fillers does not modify the overall stress versus strain behavior of the matrices. However, all the EVA grades show an increase in tensile strength and modulus with the incorporation of nanofillers (Table 2). The tensile strength has a significant decrement when the VA content is increased from 40 to 50 wt%, whereas further increase in VA content does not show any significant change in tensile strength. This change may be due to the reduction in crystallinity with VA content and at a point between 40 and 50%, the material becomes completely amorphous [29].

The addition of expanded graphite and MWCNTs has significant reinforcing effect, the maximum improvement in tensile strength and modulus being shown by the high vinyl acetate grades of EVA_{50} to EVA_{70} and exhibits least increment for EVA_{40}. This may be because of the easy dispersion of nanofillers in the rubbery phase and hence the high vinyl acetate grades disperse the fillers well. Addition of 4 wt% of EG enhances the tensile strength of EVA_{40} by 11.5%, whereas MWCNT and CNF increase it by 7 and 32.8%, respectively. On the other hand, the increments are 58, 14, and 150%, respectively, in EVA_{70}. The EVA_{40} consists of more plastic (crystalline) phase and hence the nanofillers find it more difficult to disperse and hence form relatively more agglomerations, whereas in high vinyl acetate grades, the amount of free volume is more and hence the fillers can disperse relatively easily.

The tensile strength of various nanocomposites can be related to the volume fraction of nanofiller, using the reinforcing factor, R follows:

$$\frac{\sigma_c}{\sigma_m} = 1 + R(\phi_f) \tag{3}$$

where σ_c and σ_m are the tensile strength of the composite and the virgin matrix, respectively. ϕ_f is the volume fraction of the respective filler. The relative tensile strength, $\frac{\sigma_c}{\sigma_m}$ is plotted against volume fraction of filler ϕ_f for all the three fillers with the same EVA_{50} matrix. The plots are linear fitted to obtain the reinforcing factor of each filler in the EVA_{50} matrix (Fig. 5).

These values are very close to the respective reinforcing factors calculated from Eq. 3. For example, the value of

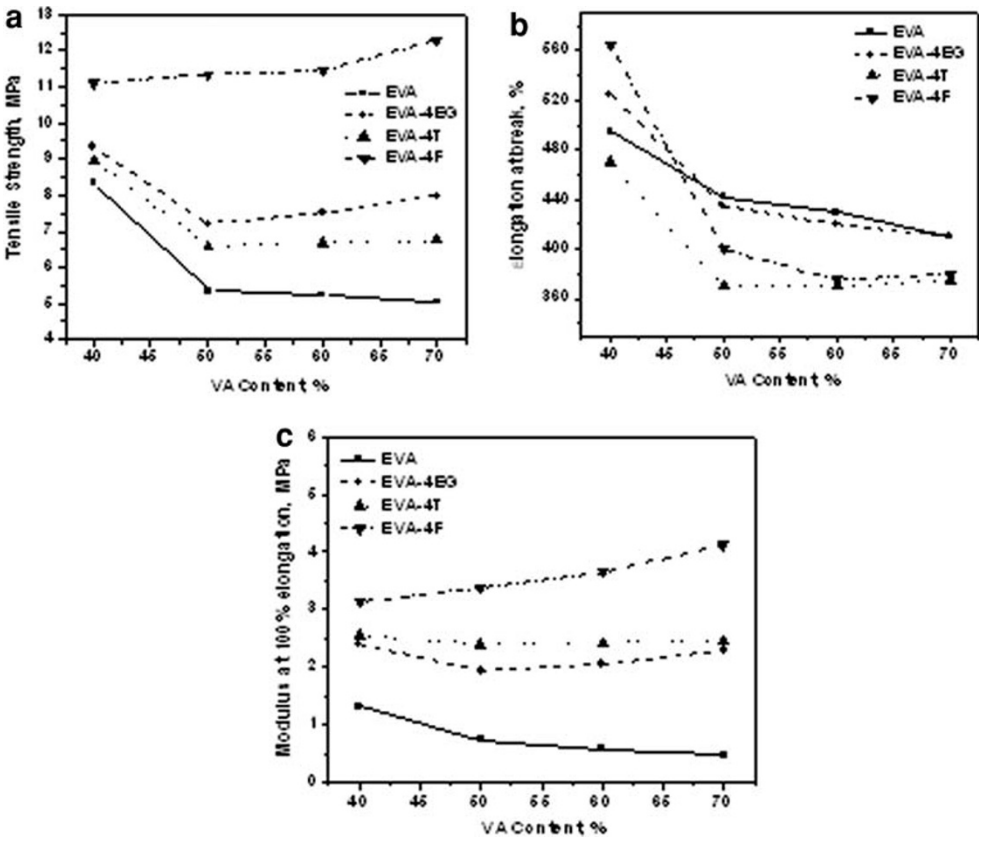

Fig. 4 Dependence of tensile properties on VA content

Table 2 Tensile properties of EVA grades and their nanocomposites at 4 wt% filler loading

Sample	Tensile strength (MPa)	Elongation at break (%)	Modulus at 100% elongation (MPa)
EVA_{40}	8.36 ± 0.19	495 ± 15	1.31 ± 0.12
EVA_{50}	5.35 ± 0.12	440 ± 10	0.74 ± 0.11
EVA_{60}	5.24 ± 0.20	430 ± 10	0.57 ± 0.05
EVA_{70}	5.04 ± 0.17	410 ± 14	0.48 ± 0.07
EVA_{40}-4EG	9.32 ± 0.18	525 ± 12	2.39 ± 0.15
EVA_{50}-4EG	7.21 ± 0.14	435 ± 16	1.94 ± 0.08
EVA_{60}-4EG	7.51 ± 0.10	420 ± 10	2.05 ± 0.06
EVA_{70}-4EG	7.98 ± 0.15	410 ± 15	2.29 ± 0.12
EVA_{40}-4T	8.95 ± 0.18	470 ± 15	2.56 ± 0.13
EVA_{50}-4T	6.60 ± 0.12	370 ± 15	2.40 ± 0.09
EVA_{60}-4T	6.68 ± 0.18	370 ± 16	2.42 ± 0.10
EVA_{70}-4T	6.75 ± 0.20	375 ± 15	2.46 ± 0.10
EVA_{40}-4F	11.10 ± 0.21	565 ± 20	3.13 ± 0.14
EVA_{50}-4F	11.34 ± 0.12	400 ± 15	3.38 ± 0.11
EVA_{60}-4F	11.45 ± 0.15	375 ± 13	3.65 ± 0.10
EVA_{70}-4F	12.30 ± 0.16	380 ± 15	4.13 ± 0.15

reinforcing factor, R, obtained by linear fitting is 0.27 for EVA_{50}-4F, which is very close to the value calculated from Eq. 3. The reinforcing factors of various EVA nanocomposites are plotted against the VA contents of EVAs in Fig. 6.

From the plots, it is clear that the reinforcing factor of EG and CNF increases in direct proportion with the VA content. The reinforcing effect of MWCNTs is lower. This might have resulted from relatively poor dispersion of MWCNT as compared to the other two fillers. It is to be

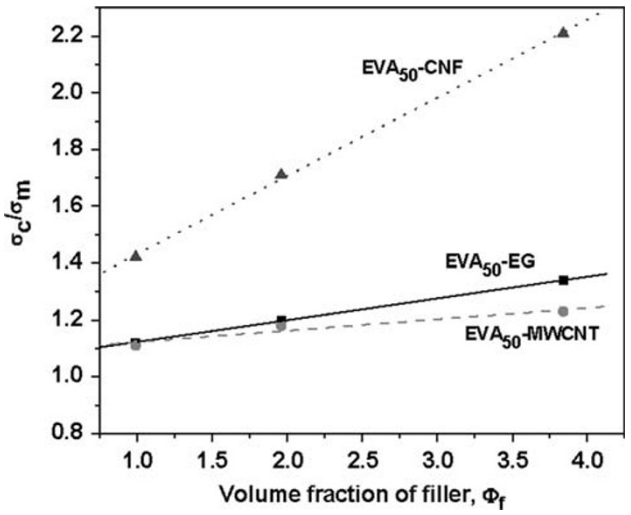

Fig. 5 $\frac{\sigma_c}{\sigma_m}$ vs. ϕ_f plots for EVA_{50}-EG, EVA_{50}-MWCNT, and EVA_{50}-CNF

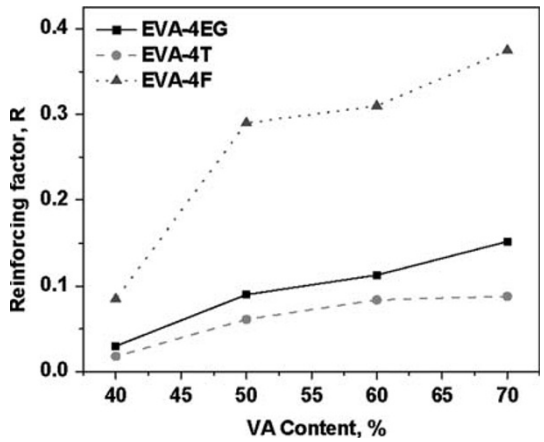

Fig. 6 Plots of reinforcing factor(R) versus VA content of EVA for EVA-4EG, EVA-4T, and EVA-4F

noted that increment is more prominent in the partially amorphous to fully amorphous transition region which occurs beyond 50% VA content.

Solvent Swelling Analysis

The solvent swelling analysis supports the results of mechanical properties. The composite samples having various nanofillers exhibit higher rubber volume fraction (V_r) values (Table 3) due to the interaction between the polymer chains and the filler. The highest value is achieved with CNFs and also when the vinyl acetate content is highest.

Differential Scanning Calorimetry

DSC studies of all the EVA copolymers and their nanocomposites have been carried out. On loading the nanofillers, there is marginal change in the enthalpy of melting (ΔH_m) values with no change in the melting peak temperature. The percentage crystallinity of all the samples lies in the range 0.3–0.4%, thus confirming that all the nanocomposites are basically amorphous materials. It has been reported earlier that loading of carbon nanotubes reduces the crystallinity of EVA having 27% VA content (much lower than those used in the present investigation) due to the reduction in the orientation of polymer chains as a result of polymer–filler interaction [30]. However, there is no such indication from the DSC traces for these amorphous polymers, as the ΔH_m values are very low.

Table 3 Rubber volume fraction of EVA grades and their nanocomposites at 4 wt% filler

Sample	Volume fraction of rubber (V_r)
EVA_{40}	0.106
EVA_{50}	0.114
EVA_{60}	0.115
EVA_{70}	0.118
EVA_{40}-4EG	0.118
EVA_{50}-4EG	0.125
EVA_{60}-4EG	0.129
EVA_{70}-4EG	0.131
EVA_{40}-4T	0.158
EVA_{50}-4T	0.187
EVA_{60}-4T	0.191
EVA_{70}-4T	0.194
EVA_{40}-4F	0.210
EVA_{50}-4F	0.280
EVA_{60}-4F	0.285
EVA_{70}-4F	0.288

Dynamic Mechanical Thermal Analysis

Dynamic mechanical thermal analysis is an excellent tool to characterize the viscoelastic properties of polymer composites. A better understanding of the dynamic mechanical properties of the composite will help to define structure/property relationships and subsequently to relate these properties to product's final performance. Figure 7a displays the variation of tan δ and storage modulus, E'(inset) with temperature and Fig. 7b–e represents the variation in T_g, storage modulus, and tan δ_{Max} with vinyl acetate content of EVA. It can be observed that while EVA_{40} exhibits a T_g of −31.6 °C the high VA-containing sample EVA_{70} exhibits T_g of −18.5 °C (Table 4). This significant shift in T_g is due to the variation of ethylene content in the copolymers (http://www.levapren.com). As the ethylene content increases, the T_g shifts to the lower

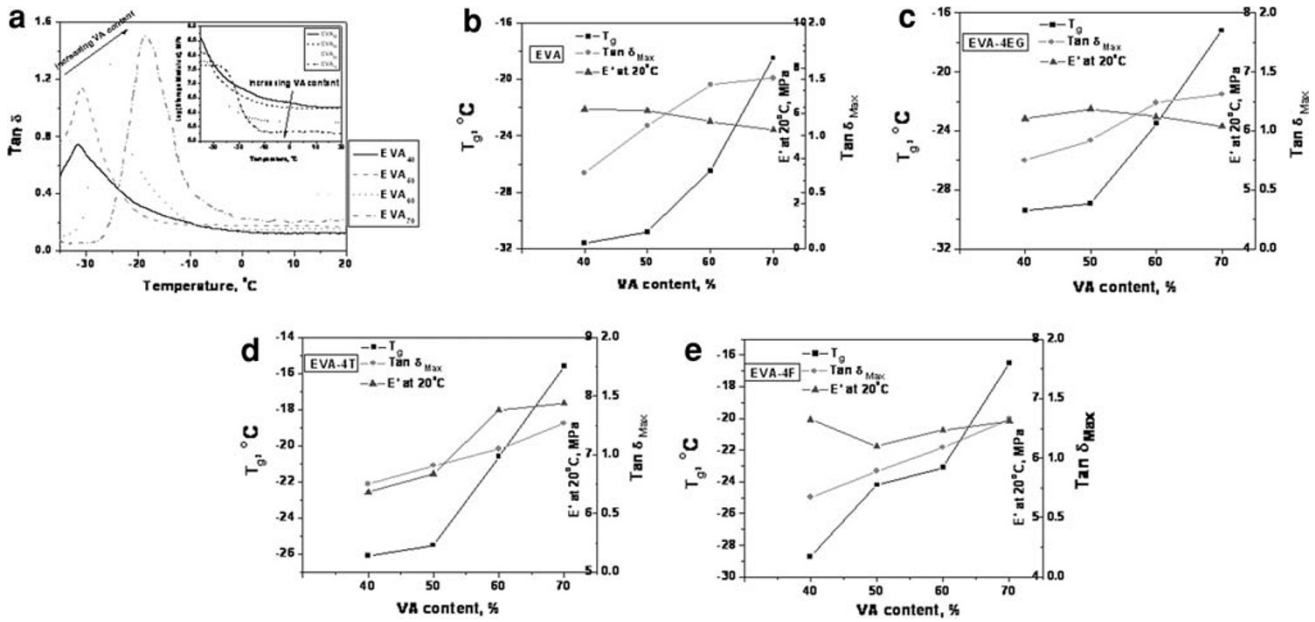

Fig. 7 **a** Variation of tan δ and storage modulus (inset) with temperature, **b**–**e** variation of T_g, E', and tan δ_{Max} with VA content

temperatures. Also, it is to be noted that the tan δ peak height reduces as the VA content reduces. This is due to increase in chain flexibility due to increasing rubbery nature. Or in other words, the amount of amorphous phase is increased with the increase of the VA content in the EVA.

As expected, various nanocomposites exhibit much higher storage modulus than pure EVA grades, especially at low temperatures, given the reinforcing effect of nanofillers on the matrix. In addition, the presence of the fillers also enables the matrix to sustain high-modulus value at high temperatures. Also, various nanocomposites show a reduction in tan δ peak height as compared to those of respective neat elastomers. This is due to the restriction in polymer chain movements employed by the filler–polymer interactions.

Table 4 DMTA data of EVA grades and their nanocomposites at 4 wt% filler loading

Sample	T_g (°C)	Storage modulus Log E' (Pa) at		tan δ at	
		T_g	20 °C	T_g	20 °C
EVA_{40}	−31.6	7.93	6.18	0.76	0.13
EVA_{50}	−30.8	7.68	6.10	1.09	0.18
EVA_{60}	−26.5	6.50	5.64	1.45	0.16
EVA_{70}	−18.5	6.03	5.27	1.51	0.21
EVA_{40}-4EG	−29.4	7.96	6.21	0.75	0.13
EVA_{50}-4EG	−28.9	7.93	6.37	0.92	0.16
EVA_{60}-4EG	−23.5	7.40	6.24	1.24	0.22
EVA_{70}-4EG	−17.2	7.25	6.08	1.31	0.22
EVA_{40}-4T	−26.1	7.52	6.36	0.75	0.12
EVA_{50}-4T	−25.5	8.21	6.68	0.91	0.17
EVA_{60}-4T	−20.6	7.16	7.76	1.05	0.13
EVA_{70}-4T	−15.6	7.41	7.88	1.27	0.20
EVA_{40}-4F	−28.7	8.08	6.65	0.67	0.12
EVA_{50}-4F	−24.2	7.56	6.20	0.89	0.16
EVA_{60}-4F	−23.1	8.12	6.47	1.09	0.19
EVA_{70}-4F	−16.5	7.78	6.62	1.33	0.21

Table 5 Thermal conductivity data of various EVA nanocomposites at 4 wt% filler loading

Sample	Thermal conductivity (W/mK)
EVA_{40}	0.22
EVA_{50}	0.24
EVA_{60}	0.23
EVA_{70}	0.24
EVA_{40}-4EG	0.71
EVA_{50}-4EG	0.83
EVA_{60}-4EG	0.87
EVA_{70}-4EG	0.89
EVA_{40}-4T	0.90
EVA_{50}-4T	1.13
EVA_{60}-4T	1.16
EVA_{70}-4T	1.18
EVA_{40}-4F	0.60
EVA_{50}-4F	0.69
EVA_{60}-4F	0.75
EVA_{70}-4F	0.78

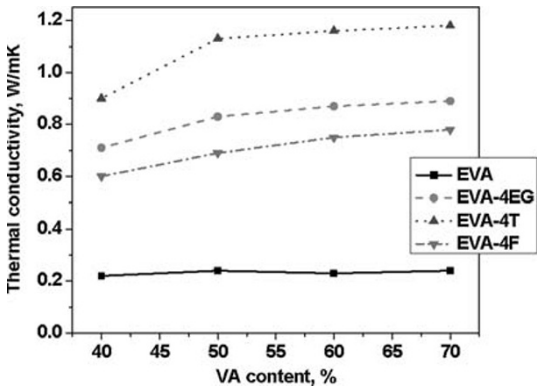

Fig. 8 Variation of thermal conductivity with VA content

Thermal Conductivity

1. The thermal conductivity of various nanocomposite samples has been analyzed in this section (Table 5 and Fig. 8). There is no significant difference among the thermal conductivity values of different EVA grades. Addition of 4 wt% of expanded graphite increases the thermal conductivity several folds over the neat elastomers. Increments are more prominent in the high VA-containing grades. Due to their inherent superior thermal conductivity, MWCNTs provide highest enhancement in thermal conductivity in various matrices. The thermal conductivity enhancement of polymer nanocomposites depends to a large extent on the thermal conductivity of nanoscale fillers and their structural properties [31]. Even though CNF has higher aspect ratio, its intrinsic thermal conductivity is about 2000 W/mK which is much lower than that of MWCNT which is 3000 W/mK [32]. In spite of the higher polymer–filler interaction revealed by V_r values, CNF-based composites register lower thermal conductivity values because of the above reason. Interfacial bonding between filler and polymer plays a vital role on the thermal conductivity of the resulting nanocomposites following earlier references [33]. In the present case, however, the MWCNT shows a relatively poorer dispersion and also the swelling resistance is lower than that of CNF-based composites. It seems that there are many factors, including the thermal conductivity of the filler, important in determining the thermal conductivity of the composites.

Thermogravimetric Analysis

Thermogravimetric analysis has been carried out to study the degradation behavior of various nanocomposites prepared (Fig. 9a–c and Table 6). The representative DTG and TGA (inset) plots of virgin EVA grades are provided in

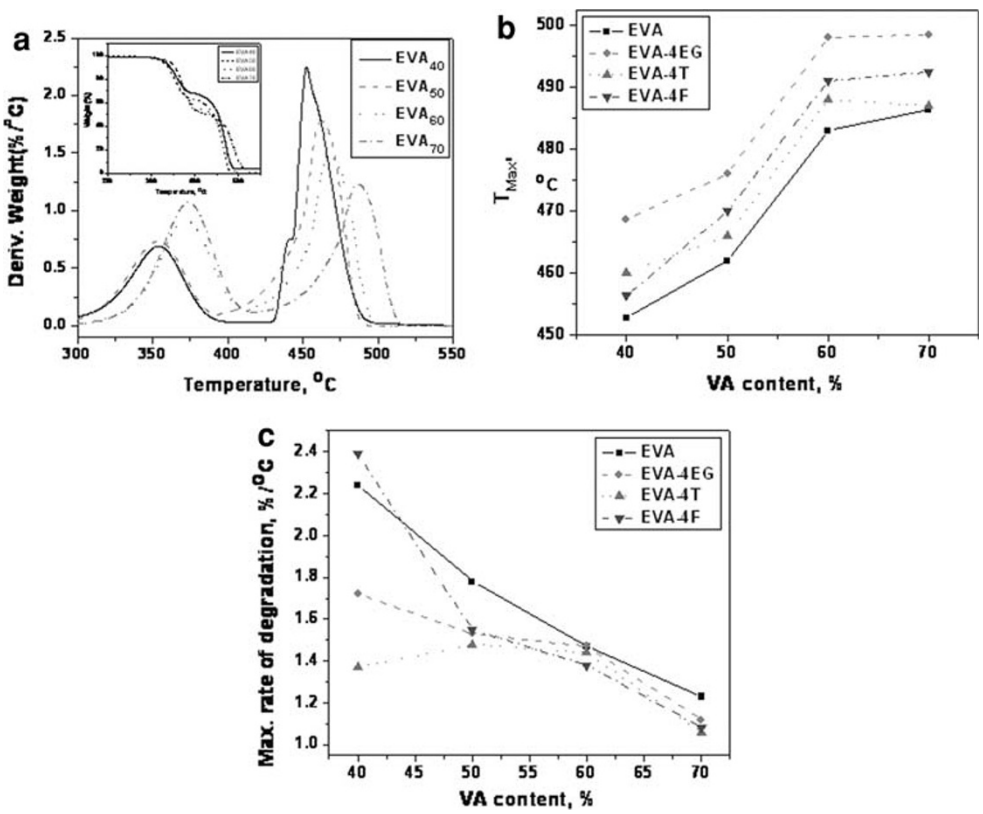

Fig. 9 **a** DTG and TGA (inset) curves of EVA grades, **b** and **c** dependence of T_{Max} and rate of degradation on VA content

Table 6 Thermal degradation data of various EVA nanocomposites at 4 wt% filler loading

Sample	T_{Max} (°C)	Maximum rate of degradation (%/°C)
EVA_{40}	453	2.24
EVA_{50}	462	1.78
EVA_{60}	483	1.47
EVA_{70}	486	1.23
EVA_{40}-4EG	469	1.72
EVA_{50}-4EG	476	1.53
EVA_{60}-4EG	498	1.47
EVA_{70}-4EG	498	1.12
EVA_{40}-4T	460	1.37
EVA_{50}-4T	466	1.48
EVA_{60}-4T	488	1.44
EVA_{70}-4T	487	1.06
EVA_{40}-4F	456	2.39
EVA_{50}-4F	470	1.55
EVA_{60}-4F	491	1.38
EVA_{70}-4F	493	1.08

Fig. 9a. Temperature corresponding to maximum rate of degradation (T_{Max}) and maximum rate of degradation for various nanocomposites are reported in Table 6. The results show that the EVA with higher VA content exhibits higher thermal stability. The weight loss in pure EVA starts around 300 °C due to the liberation of acetic acid. In presence of nanofillers, the onset of weight loss in the composites occurs at higher temperatures. The sudden weight loss observed between 400 and 500 °C due to the thermal degradation of the polymer is also shifted to higher temperatures in EVA nanocomposites. That means the heat stability of the polymer is improved in general, by the incorporation of various carbon nanofillers. Unlike the mechanical properties, the thermal stability of various nanocomposites exhibits more dependence on filler than nature of the matrix. Among the various nanofillers used, EG imparts maximum thermal degradation stability to various EVA matrices. This may be due to the flake like structure of graphite particles, which prevent easy degradation of polymer chains much effectively. The individual T_{Max} values of EG, MWCNT, and CNF are 736, 623, and 592 °C, respectively, which support the results. The higher thermal stability of EG might have played a significant role in providing EG-reinforced nanocomposites highest thermal stability.

Conclusions

Reinforcing effect of expanded graphite, multiwalled carbon nanotube, and carbon nanofiber on various elastomeric grades of EVA have been investigated and the effect of vinyl acetate content on various composite properties has been analyzed. The enhancements in mechanical, dynamic mechanical, and thermal properties indicate that the more elastomeric (VA content) the matrix is, the more easily the nanofillers get dispersed due to higher free volume. This effect is more prominent where the polymer achieves complete amorphousness which occurs between 40 and 50% VA content. Further increments in VA content did not bring about significant improvements in filler dispersion as evident from the TEM photographs. This effect is reflected in the enhancement in properties with the addition of nanofillers, though EVA_{40} exhibits highest mechanical properties as compared to the higher VA-containing grades. This trend has been followed in both dynamic mechanical properties and thermal conductivity of the nanocomposites. The thermal degradation of the nanocomposites shows more dependence on the type of nanofiller rather than the VA content of EVA. Among the three nanofillers, expanded graphite provides maximum thermal stability.

Acknowledgment The authors acknowledge the financial assistance provided by DRDO, New Delhi, India.

References

1. S.K. Datta, A.K. Bhowmick, T.K. Chaki, A.B. Majali, R.S. Despande, Polymer (Guildf) **37**, 45 (1996). doi:10.1016/0032-3861(96)81598-9
2. S.K. Datta, A.K. Bhowmick, P.G. Mukunda, T.K. Chaki, Polym. Degrad. Stab. **50**, 75 (1995). doi:10.1016/0141-3910(95)00125-6
3. M. Pramanik, S.K. Srivastava, B.K. Samantaray, A.K. Bhowmick, J. Appl. Polym. Sci. **87**, 2216 (2003). doi:10.1002/app.11475
4. M. Pramanik, S.K. Srivastava, B.K. Samantaray, A.K. Bhowmick, J. Polym. Sci. B Polym. Phys. **40**, 2065 (2002). doi:10.1002/polb.10266
5. S.K. Srivastava, M. Pramanik, H. Acharya, J. Polym. Sci. B Polym. Phys. **44**, 471 (2006). doi:10.1002/polb.20702
6. M.C. Costache, D.D. Jiang, C.A. Wilkie, Polymer (Guildf) **46**, 6947 (2005). doi:10.1016/j.polymer.2005.05.084
7. R. Prasad, R.K. Gupta, F. Cser, S.N. Bhattacharya, J. Appl. Polym. Sci. **101**, 2127 (2006). doi:10.1002/app.22331
8. F.P. La Mantia, N.T. Dintcheva, Polym. Test. **25**, 701 (2006). doi:10.1016/j.polymertesting.2006.03.003
9. W. Zhang, D. Chen, Q. Zhao, Y. Fang, Polymer (Guildf) **44**, 7953 (2003). doi:10.1016/j.polymer.2003.10.046
10. T. Kuila, H. Acharya, S.K. Srivastava, A.K. Bhowmick, J. Appl. Polym. Sci. **108**, 1329 (2008). doi:10.1002/app.27834
11. I.S. Suh, S.H. Ryu, J.H. Bae, Y.W. Chang, J. Appl. Polym. Sci. **94**, 1057 (2004). doi:10.1002/app.20962
12. C.H. Jeon, S.H. Ryu, Y.W. Chang, Polym. Int. **52**, 153 (2003). doi:10.1002/pi.1066
13. J. Sharif, W.M.Z.W. Yunus, K.H. Dahlan, M.H. Ahmad, J. Appl. Polym. Sci. **100**, 353 (2006). doi:10.1002/app.23121
14. M. Sadeghi, G. Khanbabaei, A.H.S. Dehaghani, M. Sadeghi, M.A. Aravand, M. Akbarzade, S. Khatti, J. Membr. Sci. **322**, 423 (2008). doi:10.1016/j.memsci.2008.05.077

15. M. Brogly, M. Nardin, J. Schultz, J. Appl. Polym. Sci. **64**, 1903 (1997). doi:10.1002/(SICI)1097-4628(19970606)64:10<1903::AID-APP4>3.0.CO;2-M
16. A. Arsac, C. Carrot, J. Guillet, J. Appl. Polym. Sci. **74**, 2625 (1999). doi:10.1002/(SICI)1097-4628(19991209)74:11<2625::AID-APP9>3.0.CO;2-G
17. S. Bistac, P. Kunemann, J. Schultz, Polymer (Guildf) **39**, 4875 (1998). doi:10.1016/S0032-3861(97)10328-7
18. N. Gospodinova, T. Zlatkov, L. Terlemezyan, Polymer (Guildf) **39**, 2583 (1998). doi:10.1016/S0032-3861(97)00558-2
19. S. Peeterbroeck, B. Lepoittevin, E. Pollet, S. Benali, C. Broekaert, M.D. Alexandre, P.B. Viville, R. Lazzaroni, P. Dubois, Polym. Eng. Sci. **46**, 1022 (2006). doi:10.1002/pen.20560
20. S. Peeterbroeck, M. Alexandre, J.B. Nagy, C. Pirlot, A. Fonseca, N. Moreau, G. Philippin, J. Delhalle, Z. Mekhalif, R. Sporken, G. Beyer, P. Dubois, Compos. Sci. Technol. **64**, 2317 (2004). doi:10.1016/j.compscitech.2004.01.020
21. K.-Y. Lee, K.-Y. Kim, Polym. Degrad. Stab. **93**, 1290 (2008). doi:10.1016/j.polymdegradstab.2008.04.007
22. S. Peeterbroeck, F. Laoutid, B. Swoboda, J.-M. Lopez-Cuesta, N. Moreau, J.B. Nagy, M. Alexandre, P. Dubois, Macromol. Rapid Commun. **28**, 260 (2007). doi:10.1002/marc.200600614
23. J.J. George, R. Sengupta, A.K. Bhowmick, J. Nanosci. Nanotechnol. **8**, 1913 (2008). doi:10.1166/jnn.2008.230
24. J.J. George, A.K. Bhowmick, J. Mater. Sci. **43**, 702 (2008). doi:10.1007/s10853-007-2193-6
25. J.J. George, A.K. Bhowmick, Nanoscale Res. Lett. **3**, 508 (2008). doi:10.1007/s11671-008-9188-3
26. N.C. Das, S. Maiti, J. Mater. Sci. **43**, 1920 (2008). doi:10.1007/s10853-008-2458-8
27. S. Peeterbroeck, L. Breugelmans, M. Alexandre, J.B. Nagy, P. Viville, R. Lazzaroni, P. Dubois, Compos. Sci. Technol. **67**, 1659 (2007). doi:10.1016/j.compscitech.2006.07.001
28. S. Sadhu, A.K. Bhowmick, J. Polym. Sci. B Polym. Phys. **42**, 1573 (2004)
29. A.M. Henderson, IEEE Electr. Insul. Mag. **9**, 30 (1993). doi:10.1109/57.249923
30. H.E. Miltner, S. Peeterbroeck, P. Viville, P. Dubois, B. Vanmele, J. Polym. Sci. B Polym. Phys. **45**, 1291 (2007). doi:10.1002/polb.21193
31. Y. Yang, M.C. Gupta, J.N. Zalameda, W.P. Winfree, Micro & Nano Lett **3**(2), 35 (2008). doi:10.1049/mnl:20070073
32. M.H. Al-Saleh, U. Sundararaj, Carbon **47**, 2 (2009). doi:10.1016/j.carbon.2008.09.039
33. S.T. Huxtable, D.G. Cahill, S. Shenogin, L. Xue, R. OZisik, P. Barone, M. Usrey, M.S. Strano, G. Siddons, M. Shim, P. Keblinski, Nat. Mater. **2**, 731 (2003). doi:10.1038/nmat996